Raman spectroscopy of decrespignyite $(Y,REE)_4Cu(CO_3)_4Cl(OH)_5•2(H_2O)$ and in relation with other halogenated carbonates including bastnasite, hydroxybastnasite, parisite and northupite

Ray L. Frost • **and Sara J. Palmer**

Chemistry Discipline, Faculty of Science and Technology, Queensland University of Technology, GPO Box 2434, Brisbane Queensland 4001, Australia.

ABSTRACT

Raman spectroscopy complimented with infrared spectroscopy has been used to study the rare earth based mineral decrespignyite $(Y,REE)_4Cu(CO_3)_4Cl(OH)_5•2(H_2O)$ and compared with the Raman spectra of a series of selected natural halogenated carbonates from different origins including bastnasite, parisite and northupite. The Raman spectrum of decrespignyite displays three bands are at 1056, 1070 and 1088 cm^{-1} attributed to the CO_3^{2-} symmetric stretching vibration. The observation of three symmetric stretching vibrations is very unusual. The position of CO_3^{2-} symmetric stretching vibration varies with mineral composition. Raman bands of decrespignyite show bands at 1391, 1414, 1489 and 1547 cm^{-1}. Raman spectra of bastnasite, parisite and northupite show a single band at 1433, 1420 and 1554 cm^{-1} assigned to the ν_3 $(CO_3)^{2-}$ antisymmetric stretching mode. The observation of additional Raman bands for the ν_3 modes for some halogenated carbonates is significant in that it shows distortion of the carbonate anion in the mineral structure. Four Raman bands are observed at 791, 815, 837 and 849 $cm^{-1}$and assigned to the $(CO_3)^{2-}$ ν_2 bending modes. Raman bands are observed for decrespignyite at 694, 718 and 746 cm^{-1} and are assigned to the $(CO_3)^{2-}$ ν_4 bending modes. Raman bands are observed for the carbonate ν_4 in phase bending modes at 722 cm^{-1} for bastnasite, 736 and 684 cm^{-1} for parisite, 714 cm^{-1} for northupite. Multiple bands are observed in the OH stretching region for decrespignyite, bastnasite and parisite indicating the presence of water and OH units in the mineral structure.

KEY WORDS: Decrespignyite, bastnasite, hydroxybastnasite, parisite and northupite yttrium, rare earth carbonates

• Author to whom correspondence should be addressed (r.frost@qut.edu.au)

INTRODUCTION

Decrespignyite-(Y) $(Y,REE)_4Cu(CO_3)_4Cl(OH)_5 \bullet 2(H_2O)$ is a new copper yttrium rare earth carbonate chloride hydrate from the Paratoo copper mine, near Yunta, Olary district, South Australia [1]. Decrespignyite-(Y) occurs as blue crusts, coatings and fillings in thin fissures on the slatey country rock [1]. Decrespignyite-(Y) is a supergene mineral which precipitated from mildly basic carbonated ground waters. The mineral is named after Robert Champion de Crespigny, an eminent character in the Australian mining industry and former chancellor of the University of Adelaide.

The composition of the mineral has been published [1]. The mineral is fundamentally a hydrated hydroxy chloride-carbonate of copper and yttrium with other rare earths. The mineral is a source of yttrium and other rare earths. The origin of the mineral has been delineated [2]. Some Raman and infrared spectra have been published but without band assignments [1].There are a number of halogen containing carbonates including bastnaesite (often written as bastnasite and bastnäsite) $[(Ce,La)CO_3F]$, parisite $[(Ce_2,Ca)(CO_3)F_2]$, northupite $[(Na_2,Mg)(CO_3)_2F]$, and phosgenite $[Pb_2CO_3Cl]$ [3]. In fact this group of minerals supplies more than 70% of the world's supply of rare earths. In addition minerals based upon hydroxbastnasite are also known but little or no information is available for this mineral [4-6]. It is probable that the mineral decrespignyite-(Y) is structurally related to bastnäsite-synchysite-parsite group all of which adopt a hexagonal or at least a pseudohexagonal layered structure based upon repeat units of $REE—CO_3^{2—}(F,OH)$ [7-9].

The importance of these rare earth minerals is that the minerals are a source of rare earths including lanthanum, yttrium and cerium. Bastnäsite is one of three carbonate-fluoride minerals. There is bastnäsite-(Ce) with a formula of $(Ce, La)CO_3F$. There is bastnäsite-(La) with a formula of $(La, Ce)CO_3F$. There is also bastnäsite-(Y) with a formula of $(Y, Ce)CO_3F$. Most bastnäsite is bastnäsite-(Ce), and cerium is by far the most common of the rare earths in this class of minerals. Bastnäsite is closely related to the mineral parisite; both are rare earth fluorocarbonates. Parisite formula varies depending upon the locality of origin and may be generalized as $[Ca(Ce,La,Nd)_2(CO_3)F_2]$. Bastnasite forms a series with the mineral hydroxylbastnasite. This latter mineral has a formula $[(Ce,La)CO_3(OH,F)]$ in which hydroxyl units substitute for the fluorine.

The crystal structures of most halogenated carbonates have been studied [10-12]. However the crystal structure of decrespignyite is not known or defined. The crystal structure of parisite is

said to be rhombohedral but the structure depends on the composition and origin of the mineral [10, 13-17]. The infrared spectra of bastnasite, parisite and northupite have been published [18, 19]. According to Farmer [3], bastnasite is hexagonal and the carbonate units lie on the 6(h) sites with point symmetry C_s. The internal modes of the carbonate ion are symmetrical with little evidence of splitting. In the infrared spectra, the only evidence of symmetry reduction is the appearance of a low intensity band in the ν_1 position. The infrared spectra of parisite has been said to show low site symmetry and the presence of more than one carbonate type in the unit cell. Adler and Kerr observed splitting of ν_1 and ν_4 vibrational modes [18]. Farmer states that northupite has a highly symmetrical structure and is a rare example of a carbonate with a cubic structure [3]. The structure is complex with 16 formula units in the face-centred cubic cell. As a consequence of the reduction in symmetry from D_{3h} to C_3, all bands are both infrared and Raman active.

Raman spectroscopy has proven most useful for the study of diagenetically related minerals as often occurs with carbonate minerals [20-22]. Very few spectroscopic studies of the halogenated carbonates have been forthcoming and what studies that are available are not new. Few Raman studies of any note are available. The aim of this paper is to present Raman and infrared spectra of decrespignyite and compare with other natural halogenated carbonates including bastnasite, hydroxybastnasite, parisite and northupite and to relate the Raman spectra to the structure of decrespignyite.

Experimental

Minerals

The mineral decrespignyite was supplied by the South Australian Museum and originated from Paratoo copper mine, near Yunta, Olary district, South Australia. The chemical composition of the mineral has been published [1].

Raman spectroscopy

Crystals of decrespignyite-(Y) were placed on a polished metal surface on the stage of an Olympus BHSM microscope, which is equipped with 10x, 20x, and 50x objectives. The microscope is part of a Renishaw 1000 Raman microscope system, which also includes a monochromator, a filter system and a CCD detector (1024 pixels). The Raman spectra were excited by a Spectra-Physics model 127 He-Ne laser producing highly polarised light at 633 nm and collected at a nominal resolution of 2 cm^{-1} and a precision of ± 1 cm^{-1} in the range

between 100 and 4000 cm^{-1}. Repeated acquisition on the crystals using the highest magnification (50x) was accumulated to improve the signal to noise ratio in the spectra. Spectra were calibrated using the 520.5 cm^{-1} line of a silicon wafer. Details of the technique and spectroscopy of minerals has been published [23-40].

Infrared spectroscopy

Infrared spectra were obtained using a Nicolet Nexus 870 FTIR spectrometer with a smart endurance single bounce diamond ATR cell. Spectra over the 4000–525 cm^{-1} range were obtained by the co-addition of 64 scans with a resolution of 4 cm^{-1} and a mirror velocity of 0.6329 cm/s. Spectra were co-added to improve the signal to noise ratio.

Band component analysis was undertaken using the Jandel 'Peakfit' (Erkrath, Germany) software package which enabled the type of fitting function to be selected and allowed specific parameters to be fixed or varied accordingly. Band fitting was done using a Lorentz-Gauss cross-product function with the minimum number of component bands used for the fitting process. The Lorentz-Gauss ratio was maintained at values greater than 0.7 and fitting was undertaken until reproducible results were obtained with squared correlations (r^2) greater than 0.995. Band fitting of the spectra is quite reliable providing there is some band separation or changes in the spectral profile.

Results and discussion

Spectroscopy of carbonate anion

Nakamoto *et al.* first published and tabulated the selection rules for unidenate and bidentate anions including the carbonate anion [41]. The free ion, CO_3^{2-} with D_{3h} symmetry exhibits four normal vibrational modes; a symmetric stretching vibration (ν_1), an out-of-plane bend (ν_2), a doubly degenerate asymmetric stretch (ν_3) and another doubly degenerate bending mode (ν_4). The symmetries of these modes are A_1' (R) + A_2'' (IR) + E′ (R, IR) + E′′ (R, IR) and occur at 1063, 879, 1415 and 680 cm^{-1} respectively. Generally, strong Raman modes appear around 1100 cm^{-1} due to the symmetric stretching vibration (ν_1), of the carbonate groups, while intense IR and weak Raman peaks near 1400 cm^{-1} are due to the antisymmetric stretching mode (ν_3). Infrared modes near 800 cm^{-1} are derived from the out-of-plane bend (ν_2). Infrared and Raman modes around 700 cm^{-1} region are due to the in-plane bending mode (ν_4). This mode is doubly degenerate for undistorted CO_3^{2-} groups [41]. As the carbonate groups become distorted from regular planar symmetry, this mode splits into two

components [41]. Infrared and Raman spectroscopy provide sensitive test for structural distortion of CO_3^2.

Spectroscopy

The Raman and infrared spectra of decrespignyite-(Y) over the complete wavenumber range are shown in Fig. 1a and 1b respectively. These figures show the position and relative intensities of the bands in the Raman and infrared spectra. The infrared spectrum differs from that published by Wallwork *et al.* [1]. The Raman and infrared spectra of decrespignyite-(Y) over the 850 to 1250 cm^{-1} range are displayed in Fig. 2a and 2b. In the Raman spectrum three bands are observed at 1056, 1070 and 1088 cm^{-1}. These bands are assigned to the CO_3^{2-} ν_1 symmetric stretching mode. The observation of three bands supports the concept of three non-equivalent carbonate unit in the decrespignyite-(Y) structure. Wallwork *et al.* also observed three bands at 1062, 1075 and 1094 cm^{-1}. However no band assignments were made. These researchers [1] suggested that the reason for the three symmetric stretching modes were due to three different sites of the carbonate anion in the structure with slightly different symmetries. The infrared spectrum of decrespignyite (Fig. 2b) clearly shows a series of overlapping bands. The broad feature at 1090 cm^{-1} corresponds to the three bands in the infrared spectrum. A comparison may be made with the other rare earth chlorinated carbonates.

The Raman spectra of bastnasite is characterised by a single intense band at 1096 cm^{-1} for the Pakistan mineral and 1085 cm^{-1} for the mineral from Canada. The position of the band for the bastnasite from Norway is 1097 cm^{-1}. The variation of the band position is a function of the chemical composition of the mineral. Farmer (page 278) clearly shows the variation of the symmetric stretching mode as a function of the cation ionic radius [3]. Fundamentally the higher the ionic radius the lower the wavenumber of the symmetric stretching mode. It is proposed that the three symmetric stretching modes of the carbonate anion in the decrespignyite structure are due to the presence of different adjacent cations. The Raman spectrum of parisite [9] shows two intense bands centred at 1088 cm^{-1}. Evidence of splitting of this band is observed. Two bands are observed at 1086.5 and 1090.5 cm^{-1}; a result which is in agreement with the results for the infrared spectra of parisite where two bands at 1088 and 1078 cm^{-1} were observed [18].

Two low intensity Raman bands are observed for decrespignyite at 925 and 954 cm^{-1} and are assigned to hydroxyl deformation modes. It is interesting that in the infrared spectrum the

most intense bands are observed at 975, 1003 and 1032 cm^{-1}. These bands are also assigned to the OH deformation modes. Such bands are expected to be of low intensity in the Raman spectrum but intense in the infrared spectrum.

The Raman and infrared spectra of decrespignyite-(Y) over the 1250 to 1750 cm^{-1} range are displayed in Fig. 3a and 3b. Raman bands of decrespignyite in the 1250 to 1750 cm^{-1} region occur at 1391, 1414, 1489 and 1547 cm^{-1}. These bands are assigned to the CO_3^{2-} ν_3 antisymmetric stretching mode. The observation of four bands fits well with the observation of three bands in the symmetric stretching region in the Raman spectrum. Very low intensity Raman bands were also observed by Wallwork *et al.* but were not defined [1]. The infrared spectrum (Fig. 3b) shows even more complexity. Infrared bands are observed at 1367, 1395, 1421, 1473, 1491 and 1549 cm^{-1} and are assigned to the CO_3^{2-} ν_3 antisymmetric stretching modes. In the Raman spectrum of bastnasite from Pakistan two low intensity bands are observed at 1504 and 1432 cm^{-1}. These bands are assigned to the ν_3 $(CO_3)^{2-}$ antisymmetric stretching mode. For the Canadian bastnasite only a very low intensity band at 1433 cm^{-1} is observed and for the bastnasite from Norway a band at 1445 cm^{-1} is observed. For the parisite mineral a low intensity broad band at 1420 cm^{-1} is found [9]. Adler and Kerr reported a single band at 1443 cm^{-1} for bastnasite and 1449 cm^{-1} for parisite [18]. In the Raman spectrum of northupite a low intensity band at 1554 cm^{-1} is observed [9]. Adler and Kerr reported an infrared band at 1464 cm^{-1} [18]. The fact that only a single band is observed for northupite in the antisymmetric stretching position supports the conclusion that the symmetry of the carbonate anion in the northupite structure is preserved. Otherwise multiple bands in the antisymmetric stretching region would be observed. In the work of Hong *et al.* in the Raman spectra of fluorinated carbonates, ν_3 asymmetric stretching modes were observed at 1538 and 1525 cm^{-1} for one sample and at 1516 and 1461 cm^{-1} for a second sample [42].

In the Raman spectrum of decrespignyite (Fig. 3a) two bands are observed at 1620 and 1645 cm^{-1} and are assigned to water bending vibrations. The first band is attributed to weakly hydrogen bonded water molecules and the second band is assigned to strongly hydrogen bonded water. In the infrared spectrum three bands are found at 1605, 1635 and 1682 cm^{-1}. These bands are attributed to non or weakly hydrogen bonded water, strongly hydrogen bonded water and very strongly hydrogen bonded water molecules. Wallwork *et al.* [1] found a bending mode in the infrared spectrum at 1646 cm^{-1}.

188 The Raman spectrum of decrespignyite-(Y) over the 650 to 900 cm^{-1} range and the infrared
189 spectrum in the 600 to 850 cm^{-1} region are displayed in Fig. 4a and 4b. The complexity of
190 the carbonate symmetric stretching region is reflected in the carbonate bending region. Four
191 bands are observed at 791, 815, 837 and 849 cm^{-1}. These bands are assigned to the $(CO_3)^{2-}$ ν2
192 bending modes. In the infrared spectrum, bands are observed at 776, 787 and 800 cm^{-1}.
193 Wallwork *et al.* [1] also observed complexity in this spectral region; however no bands were
194 defined or assigned. In contrast the Raman band for bastnasite is asymmetric and two bands
195 may be resolved at 865 and 845 cm^{-1}. For the mineral hydroxybastnasite, the symmetry is
196 reduced and two low intensity bands are observed at 798 and 779 cm^{-1}. The ν_2 bending mode
197 is readily observed at 873 cm^{-1} for the parisite mineral sample. In contrast for the two USA
198 parisite mineral samples two distinct bands are observed at around 866 and 844 cm^{-1}. For the
199 mineral northupite a single very intense Raman band at 879 cm^{-1} is observed. This band
200 position is in excellent agreement with that reported by Adler and Kerr [18].One conclusion that
201 can be made is that the observation of one or more bending modes depends on the chemical
202 composition of the halogenated carbonate.

203 Raman bands are observed for decrespignyite at 694, 718 and 746 cm^{-1} and are assigned to
204 the $(CO_3)^{2-}$ ν_4 bending modes. Infrared bands are observed at 645, 678, 692, 724 and 745 cm^{-1}
205 and are attributed to this vibrational mode. The Raman band observed at 729 cm^{-1} for the
206 bastnasite is assigned to the ν_4 bending mode. Farmer in his treatise shows that there is a
207 relationship between the position of the ν_4 mode and the ionic radius of the cation in the
208 carbonate structure [3]. The variation in the position of the ν_4 band reflects the composition of
209 the bastnasite. Two bands are observed for hydroxybastnasite at 602 and 569 cm^{-1}. Whether
210 these bands are ascribable to the ν_4 mode is uncertain. For the parisite mineral multiple bands
211 are observed in the ν_4 region. Bands are observed at 789, 736, 739 and 712 cm^{-}1. In the
212 Raman spectrum of bastnasite a very low intensity band is observed at 735 (Pakistan) and
213 719 cm^{-1} (Canada). Two Raman bands are observed for the parisite mineral sample at 682
214 and 742 cm^{-1}. In the infrared spectrum of northupite a low intensity band at 714 cm^{-1} is
215 observed. Adler and Kerr also determined a band at 711 cm^{-1} for northupite [18]. This band is
216 assigned to the ν_4 bending mode. A comparison of this spectral region may be made with
217 other carbonate minerals. For rosasite a number of infrared bands are observed at 776, 748
218 and 710 cm^{-1}. These bands are assigned to the ν_4 $(CO_3)^{2-}$ bending modes. In the Raman
219 spectrum, bands are observed at 751 and 719 cm^{-1}. For malachite two infrared bands are
220 observed at 748 and 710 cm^{-1} which are assigned to this ν_4 $(CO_3)^{2-}$ bending vibration [43, 44].

Another mineral with similar formulation to rosasite, hydrozincite has infrared bands in this region at 738 and 710 cm^{-1}. The infrared spectrum of hydrocerrusite has ν_4 $(CO_3)^{2-}$ bending modes at 700, 687 and 676 cm^{-1}.The far low wavenumber region is displayed in Fig. 5. Significant intense bands are observed. This spectral region is where the chloride stretching modes would be expected.

The Raman spectrum of decrespignyite-(Y) over the 3200 to 3800 cm^{-1} range and the infrared spectrum in the 3000 to 3800 cm^{-1} region are displayed in Fig. 6a and 6b. In the Raman spectrum there appears to be two sets of bands: those centred upon 3460 cm^{-1} and those in the 3600 to 3700 cm^{-1} region. The Raman bands at 3417 and 3464 cm^{-1} are assigned to water stretching vibrations and correspond to the water bending mode at 1645 cm^{-1}. In the infrared spectrum, intense bands are observed at 3228, 3364, 3419 cm^{-1} and are attributed to water stretching bands. Raman bands observed at 3627 and 3686 cm^{-1} are attributed to OH stretching vibrations of the hydroxyl units in the decrespignyite structure. Infrared bands are observed at 3619, 3649, 3669 and 3691 cm^{-1}. Wallwork *et al.* [1] found OH stretching bands at 3419 and 3463 cm^{-1}. In their Raman spectrum bands are also observed at higher wavenumbers but were not defined. In the infrared spectrum of decrespignyite a sharp band at 3416 cm^{-1} superimposed on a broad spectral profile was observed.

The Raman spectrum of bastnasite displays bands in similar positions at 3651, 3620, 3526, 3355, 3276, 3169 and 3203 cm^{-1}. The three higher wavenumber bands (3651, 3620, 3526 cm^{-1}) are most likely assignable to OH stretching vibrations. Raman spectra of a Chinese bastnasite have been published but no spectral information is available for comparison in this spectral region [45]. Another study reported some Raman data for rare earth carbonates [42, 46]. However no spectral information in the OH stretching region was reported. The Raman spectrum of the hydroxybastnasite shows several bands at 3741, 3535, 3430, 3352 and 3317 cm^{-1}. For this mineral OH units replace F in a complex structure. It is possible that all of this set of bands is attributable to OH stretching vibrations. Aleksandrov described two types of bastnasites namely fluorobastnasite and hydroxybastnasite [47]. Another paper described the IR spectra in this spectral region with no detail except to state bands were observed [6]. For the mineral parisite broad bands in the OH stretching region are observed. Four Raman bands are observed at 3661, 3517, 3316 and 3180 cm^{-1}.

Conclusions

Halogenated carbonates especially decrespignyite-(Y), bastnasite and parisite are used for the production of metals such as Ce, La and Y. Raman spectroscopy has been used to characterise the mineral decrespignyite and a comparison made with other halogenated carbonates including bastnasite, hydroxybastnasite, parisite and northupite. The spectra of the minerals are dependent upon the mineral origin and its formulation. The halogenated carbonates are characterised by $(CO_3)^{2-}$ symmetric stretching modes in the 1078 to 1090 cm^{-1} range. In the case of decrespignyite three Raman bands are found suggesting three non-equivalent $(CO_3)^{2-}$ units in the decrespignyite structure. This concept is supported by the observation of multiple bands in the antisymmetric stretching region. Raman bands of decrespignyite occur at 1391, 1414, 1489 and 1547 cm^{-1}. These bands are assigned to the CO_3^{2-} ν_3 antisymmetric stretching mode. Two low intensity bands at 1504 and 1432 cm^{-1} for bastnasite are assigned to the ν_3 $(CO_3)^{2-}$ antisymmetric stretching mode.

The complexity of the symmetric stretching region is reflected in the $(CO_3)^{2-}$ bending region. Four Raman bands for decrespignyite are observed at 791, 815, 837 and 849 cm^{-1} and are assigned to the $(CO_3)^{2-}$ ν_2 bending modes. Two Raman bands at 865 and 845 cm^{-1} for bastnasite are assigned to the ν_2 $(CO_3)^{2-}$ bending mode. Raman bands are observed for decrespignyite at 694, 718 and 746 cm^{-1} and are assigned to the $(CO_3)^{2-}$ ν_4 bending modes.

Raman spectroscopy shows both the presence of water and OH units in certain selected minerals from this group even though the suggested formula does not show any OH units being present. The Raman spectra of bastnasite show bands at 3651, 3620, 3526, 3355, 3276, 3169 and 3203 cm^{-1}. For the mineral parisite broad bands in the OH stretching region with bands observed at 3516, 3310 and 3178 cm^{-1}. For parisite four Raman bands are observed at 3661, 3517, 3316 and 3180 cm^{-1}. A generalised formula may be written as $[Ca(Ce,La,Nd)_2(CO_3)F_2]$. Raman spectroscopy suggests a general formula $[(Ce,La)CO_3(OH,F).xH_2O]$.

Raman spectroscopy supports the concept that the position of the $(CO_3)^{2-}$bands is a function of the chemical composition of the halogenated mineral. Farmer (pp 278) showed that the $(CO_3)^{2-}$ symmetric stretching band varied according to the ionic radius of the cation [3]. Raman spectroscopy supports the concept that the symmetry of the carbonate anion is maintained in the structure of bastnasite, parisite and northupite, even though many minerals

have significant amounts of Ce, La or Y in the formula. The carbonate anion in the mineral hydroxybastnasite is of lower symmetry.

Acknowledgments

The financial and infra-structure support of the Queensland University of Technology, Chemistry discipline is gratefully acknowledged. The Australian Research Council (ARC) is thanked for funding the instrumentation. Mr Dermot Henry of Museum Victoria is thanked for the loan of the carbonate minerals, namely bastnasite, hydroxybastnasite, parisite and northupite. Mr Ben Henry from The South Australian Museum is thanked for the loan of the decrespignyite mineral.

REFERENCES

[1] K. Wallwork, U. Kolitsch, A. Pring, L. Nasdala, *Min. Mag.* **2002,** *66,* 181.

[2] J. Brugger, J. Ogierman, A. Pring, H. Waldron, U. Kolitsch, *Min. Mag.* **2006,** *70,* 609.

[3] V. C. Farmer, Mineralogical Society Monograph 4: The Infrared Spectra of Minerals, 1974.

[4] Z. Maksimovic, G. Panto, *Bulletin – Acad. Serbe des Sc.,* **1987,** *27,* 15.

[5] H. Wakita, S. Kinoshita, *Bull. Chem. Soc. Japan* **1979,** *52,* 428.

[6] Z. Maksimovic, G. Panto, *Min. Mag.* **1985,** *49,* 717.

[7] R. L. Frost, M. J. Dickfos, *Spectrochim. Acta,* **2008,** *71A,* 143.

[8] R. L. Frost, M. Dickfos, *Polyhedron* **2007,** *26,* 4503.

[9] R. L. Frost, M. J. Dickfos, *J. Raman Spectrosc.* **2007,** *38,* 1516.

[10] G. Donnay, J. D. H. Donnay, *Amer. Min.* **1953,** *38,* 932.

[11] T. Watanabe, *Scientific Papers Inst.Phys. Chem. Res. (Japan)* **1933,** *21,* 40.

[12] H. Shiba, T. Watanabe, *Compt. rend.* **1931,** *193,* 1421.

[13] D. Meng, X. Wu, T. Mou, D. Li, *Can. Min.* **2001,** *39,* 1713.

[14] D. Meng, X. Wu, M. Tao, D. Li, *Min. Mag.* **2001,** *65,* 797.

[15] Y. Ni, J. E. Post, J. M. Hughes, *Amer. Min.* **2000,** *85,* 251.

[16] D. Meng, X. Wu, G. Yang, Z. Pan, *Kuang. Xue.***1995,** *15,* 378.

[17] X. Wu, G. Yang, Z. Pan, *Kuang. Xue.***1993,** *13,* 214.

[18] H. H. Adler, P. F. Kerr, *Amer. Min.* **1963,** *48,* 839.

[19] M. V. Akhmanova, L. P. Orlova, *Geokhimiya* **1966,** 571.

[20] R. L. Frost, S. Bahfenne, *J. Raman Spectrosc.* **2011,** *42,* 219.

[21] R. L. Frost, S. Bahfenne, J. Cejka, J. Sejkora, J. Plasil, S. J. Palmer, E. C. Keeffe, I. Nemec, *J. Raman Spectrosc.* **2011,** *42,* 56.

[22] S. J. Palmer, R. L. Frost, *J. Raman Spectrosc.* **2011,** *42,* 224.

[23] S. Bahfenne, R. L. Frost, *J. Raman Spectrosc.* **2010,** *41,* 329.

[24] S. Bahfenne, R. L. Frost, *J. Raman Spectrosc.* **2010,** *41,* 465.

[25] J. Cejka, S. Bahfenne, R. L. Frost, J. Sejkora, *J. Raman Spectrosc.* **2010,** *41,* 74.

[26] J. Cejka, J. Sejkora, J. Plasil, S. Bahfenne, S. J. Palmer, R. L. Frost, *J. Raman Spectrosc.* **2010,** *41,* 459.

[27] R. L. Frost, S. Bahfenne, *J. Raman Spectrosc.* **2010,** *41,* 207.

[28] R. L. Frost, S. Bahfenne, *J. Raman Spectrosc.* **2010,** *41,* 325.

[29] R. L. Frost, S. Bahfenne, *J. Raman Spectrosc.* **2010,** *41,* 1353.

[30] R. L. Frost, S. Bahfenne, J. Cejka, J. Sejkora, S. J. Palmer, R. Skoda, *J. Raman Spectrosc.* **2010,** *41,* 690.

[31] R. L. Frost, S. Bahfenne, J. Cejka, J. Sejkora, J. Plasil, S. J. Palmer, *J. Raman Spectrosc.* **2010,** *41,* 814.

[32] R. L. Frost, S. Bahfenne, J. Cejka, J. Sejkora, J. Plasil, S. J. Palmer, *J. Raman Spectrosc.* **2010,** *41,* 1348.

[33] R. L. Frost, S. Bahfenne, E. C. Keeffe, *J. Raman Spectrosc.* **2010,** *41,* 1489.

[34] R. L. Frost, K. H. Bakon, S. J. Palmer, *J. Raman Spectrosc.* **2010,** *41,* 78.

[35] R. L. Frost, J. Cejka, J. Sejkora, J. Plasil, S. Bahfenne, S. J. Palmer, *J. Raman Spectrosc.* **2010,** *41,* 571.

[36] R. L. Frost, J. Cejka, J. Sejkora, J. Plasil, S. Bahfenne, S. J. Palmer, *J. Raman Spectrosc.* **2010,** *41,* 566.

[37] R. L. Frost, S. J. Palmer, L.-M. Grand, *J. Raman Spectrosc.* **2010,** *41,* 791.

[38] R. L. Frost, S. J. Palmer, L.-M. Grand, *J. Raman Spectrosc.* **2010,** *41,* 1507.

[39] R. L. Frost, S. J. Palmer, E. C. Keeffe, *J. Raman Spectrosc.* **2010,** *41,* 1479.

[40] R. L. Frost, J. Sejkora, E. C. Keeffe, J. Plasil, J. Cejka, S. Bahfenne, *J. Raman Spectrosc.* **2010,** *41,* 202.

[41] K. Nakamoto, J. Fujita, S. Tanaka, M. Kobayashi, *J. Amer. Chem. Soc.* **1957,** *79,* 4904.

[42] W. Hong, S. He, S. Huang, Y. Wang, H. Hou, X. Zhu, *Guang. Fenxi* **1999,** *19,* 546.

[43] R. L. Frost, W. N. Martens, L. Rintoul, E. Mahmutagic, J. T. Kloprogge, *J. Raman Spectrosc.* **2002,** *33,* 252.

[44] R. L. Frost, Z. Ding, J. T. Kloprogge, W. N. Martens, *Thermochim. Acta* **2002,** *390,* 133.

[45] H. Fan, K. Tao, Y. Xie, K. Wang, *Yanshi Xue.* **2003,** *19,* 169.

[46] W. Hong, S. He, S. Huang, Y. Wang, H. Hou, X. Zhu, *Guang. Fenxi* **1999,** *19,* 546.

[47] I. V. Aleksandrov, V. I. Ivanov, L. A. Sin'kova, *Zap. Vser. Min. Ob.* **1965,** *94,* 323.

List of Figures

368

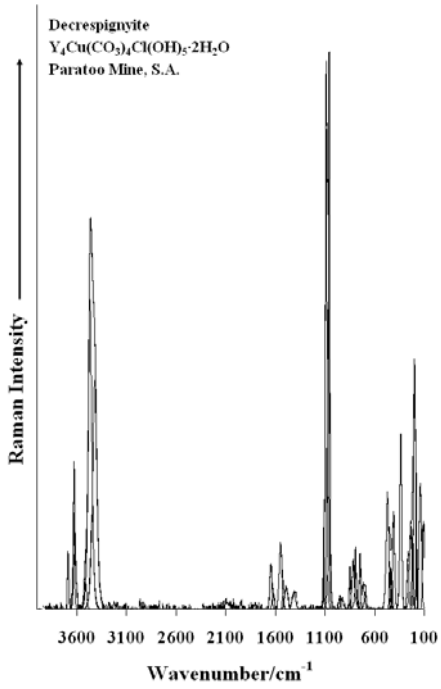

Figure 1a

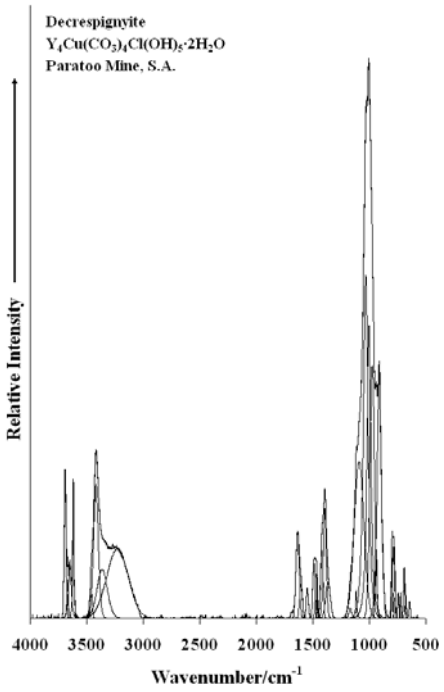

Figure 1b

369

370

371

372

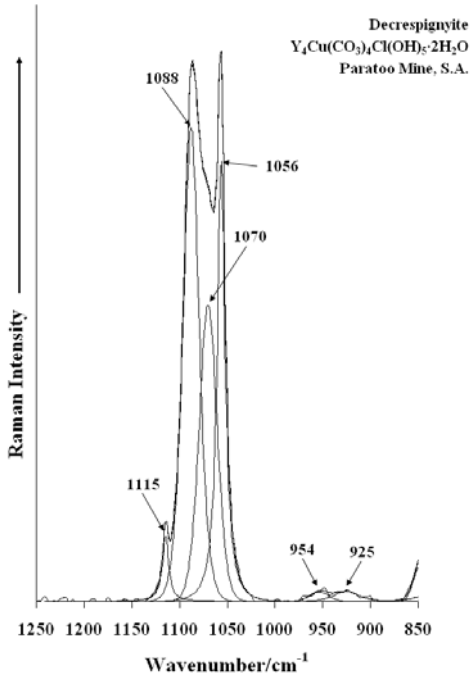

Figure 2a

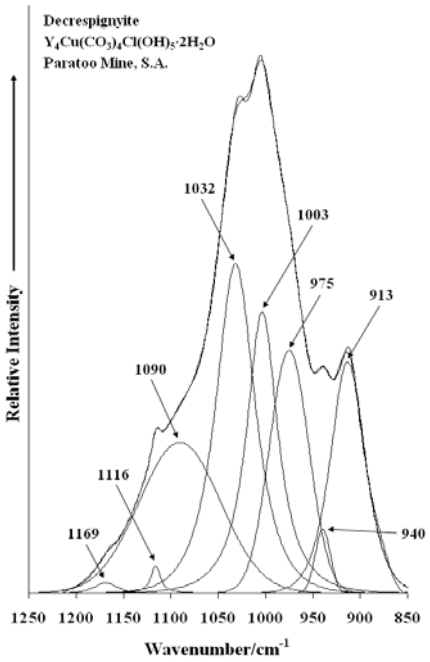

Figure 2b

373

374

375

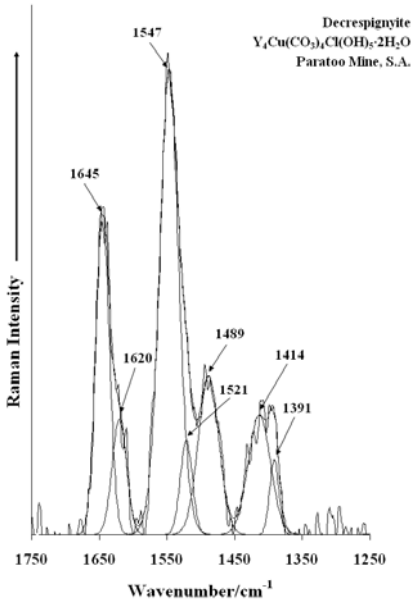

Figure 3a

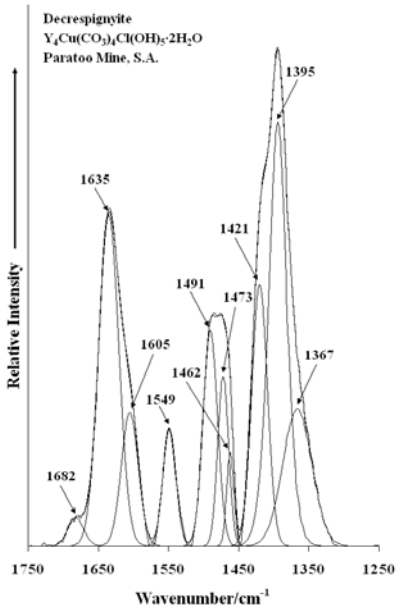

Figure 3b

376

377

378

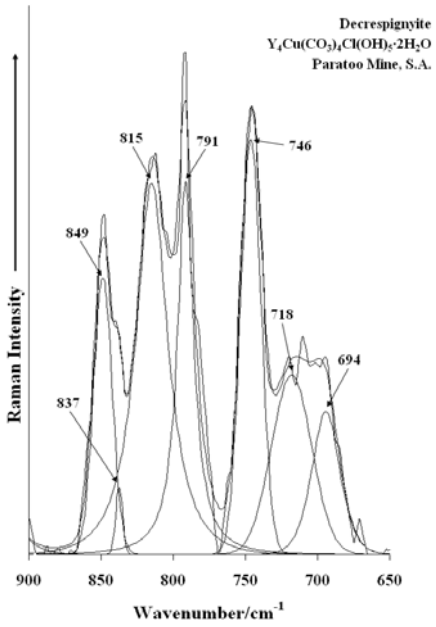

Figure 4a

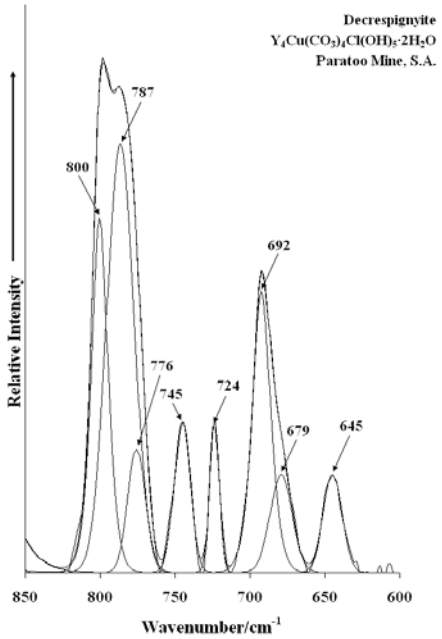

Figure 4b

379

380

381

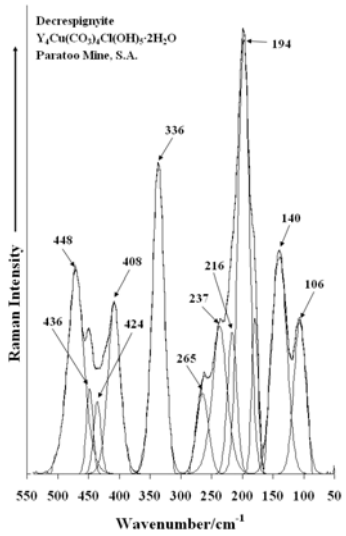

Figure 5

382

383

384

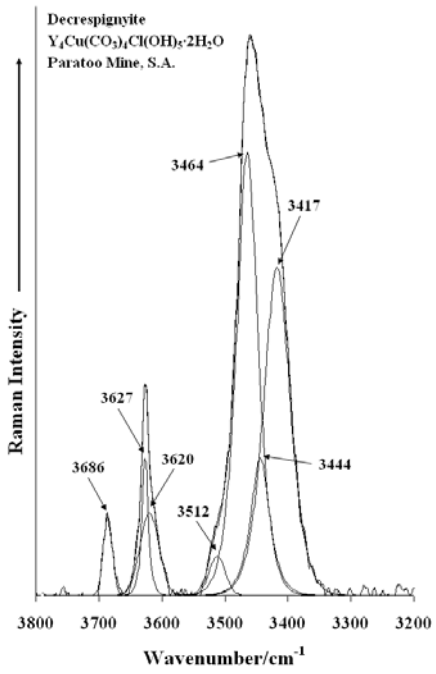

Figure 6a

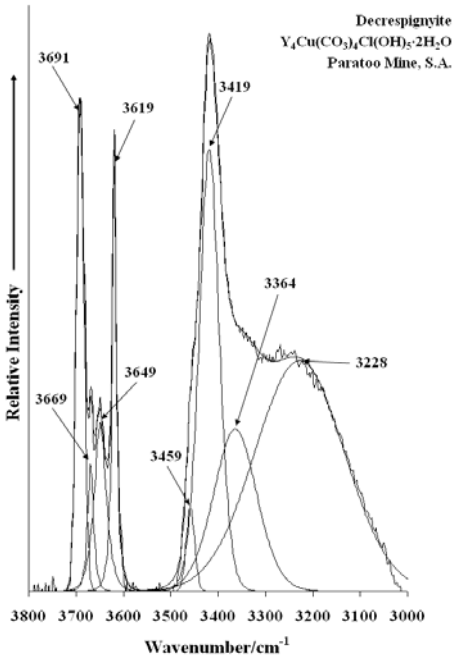

Figure 6b

385

386

387

388